

Optical Power Screening Effects in Ge-on-Si Vertical Pin Photodetectors

Original

Optical Power Screening Effects in Ge-on-Si Vertical Pin Photodetectors / Alasio, Matteo; Franco, Paolo; Tibaldi, Alberto; Bertazzi, Francesco; Namnabat, Soha; Adams, Donald; Gothoskar, Prakash; Masini, Gianlorenzo; Forghieri, Fabrizio; Ghione, Giovanni; Goano, Michele. - STAMPA. - 1005:(2023), pp. 155-159. (Intervento presentato al convegno 53rd Annual Meeting of the Italian Electronics Society tenutosi a Pizzo Calabro nel 7-9 Settembre 2022) [10.1007/978-3-031-26066-7_24].

Availability:

This version is available at: 11583/2976613 since: 2023-03-06T12:59:42Z

Publisher:

Springer

Published

DOI:10.1007/978-3-031-26066-7_24

Terms of use:

This article is made available under terms and conditions as specified in the corresponding bibliographic description in the repository

Publisher copyright

Springer postprint/Author's Accepted Manuscript

This version of the article has been accepted for publication, after peer review (when applicable) and is subject to Springer Nature's AM terms of use, but is not the Version of Record and does not reflect post-acceptance improvements, or any corrections. The Version of Record is available online at: http://dx.doi.org/10.1007/978-3-031-26066-7_24

(Article begins on next page)

Optical power screening effects in Ge-on-Si vertical *pin* photodetectors

Matteo G. C. Alasio¹[0000-0002-5175-2769], Paolo Franco¹, Alberto Tibaldi^{1,2}[0000-0002-0157-8512], Francesco Bertazzi¹[0000-0002-9409-4807], Soha Namnabat³, Donald Adams³, Prakash Gothoskar³, Gianlorenzo Masini³, Fabrizio Forghieri³, Giovanni Ghione¹[0000-0002-2362-6458], and Michele Goano^{1,2}[0000-0003-2870-1549]

¹ Dipartimento di Elettronica e Telecomunicazioni, Politecnico di Torino, Corso Duca degli Abruzzi 24, 10129 Torino, Italy

matteo.alasio@polito.it

² IEIIT-CNR, Corso Duca degli Abruzzi 24, 10129 Torino, Italy

³ Cisco Systems, 7540 Windsor Drive, Suite 412, Allentown, PA 18195, USA

Abstract. We present an experimental and numerical study on the effects of the input optical power on the electro-optic frequency response of a Ge-on-Si vertical *pin* waveguide photodetector. Experimental results were provided by Cisco Systems, which characterized several nominally identical devices. Increasing the optical power from -2 dBm to 3 dBm, a significant decrease of the electro-optic frequency response was observed in the O-band, from about 40 GHz down to approximately 32 GHz. This trend is accurately predicted by our 3D multiphysics model, where Maxwell's equations are solved with the FDTD method to evaluate the spatial distribution of photogenerated carriers, which is then converted in an optical generation rate included in the drift-diffusion solver. The 3D model provides a detailed explanation of the experiments by showing the effects of carrier screening on the magnitude of the electric field profile, which is reduced for high optical power, slowing the photogenerated carriers and reducing the bandwidth.

Keywords: Silicon photonics · Device multiphysics modeling · Ge-on-Si waveguide photodetectors · Waveguide photodetectors · Germanium · 3D modeling.

1 Introduction

We have investigated, both experimentally and through multiphysics numerical simulation, the behavior of a Ge-on-Si waveguide photodetector with vertical *pin* junction for increasing input optical power. A 3D perspective view and a cross-section of the device are shown in Fig. 1, while the main geometrical parameters are reported in Table 1. The metallic contacts are placed on top of the Ge absorber and laterally on the Si substrate. High dopant densities are present both in the substrate and at the metal/Ge interface, while most of Ge is undoped. An

optical waveguide is connected to the silicon substrate with a tapered transition, and the light is evanescently coupled in the Ge absorber [2].

This kind of photodetector, widely employed in silicon photonics [8], is commonly operated at input optical powers in the μW range. We have studied the extent of the performance drop when increasing the input optical power to the mW range, observing a reduction in the electro-optic frequency response bandwidth [4, Sec. 4.9] of more than 20%.

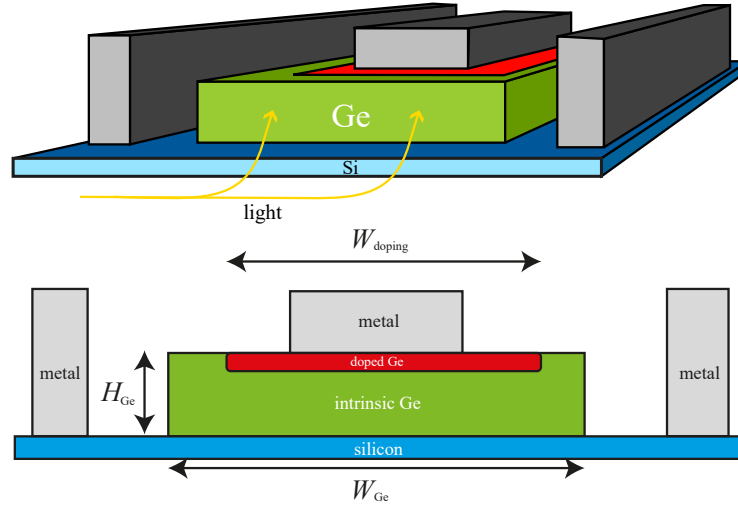


Fig. 1. Perspective view of the waveguide photodetector (top) and its transverse cross section (bottom). The Ge absorber, of length L_{Ge} , is grown over an highly doped Si substrate. The metallic contacts are placed laterally on Si and on top of the Ge absorber, where a highly doped region is present.

Table 1. Photodetector geometry.

W_{Ge}	H_{Ge}	L_{Ge}	W_{doping}
$4 \mu\text{m}$	$0.8 \mu\text{m}$	$15 \mu\text{m}$	$3 \mu\text{m}$

2 Methodology

We adopt a multiphysics approach to solve the optical and electrical problems with the finite-difference time-domain (FDTD) method and the drift-diffusion model, respectively, as implemented in Synopsys RSoft FullWAVE [11] and in the Synopsys TCAD Sentaurus suite [10]. The simulation process, whose flow

is reported in Fig. 2, and the adopted model parameters are discussed in [7]. The optical generation rate G_{opt} , evaluated by solving Maxwell’s equations, is included as a source term in the electrical transport problem. Due to the evanescent coupling of the light in the absorber, this source term has a complex spatial distribution along the device, and a 3D representation is needed [1].

This work is focused on the O-band of optical communications, centered around $\lambda = 1.31 \mu\text{m}$, where the absorption of Ge is higher [9] and the device performance is expected to be significantly more sensitive to the input optical power than in the C-band.

The experimental setup used in Cisco Systems is based on a Keysight LCA [6], which allows electro-optic measurements up to 50 GHz. Five nominally identical photodetectors, taken from different wafer regions, were characterized, determining mean value and standard deviation of the electro-optic cutoff frequency at different input optical powers for all the samples.

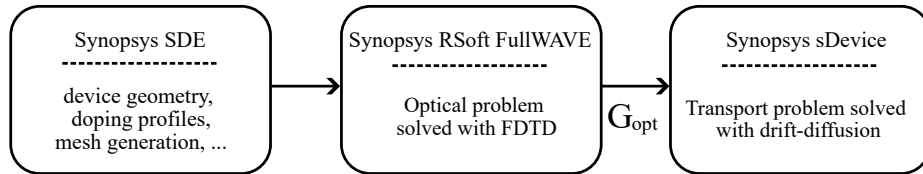


Fig. 2. Block diagram of the simulation flow in the modeling process. First, we define the device geometry, doping distributions and mesh. Then we use FDTD to extract the 3D spatial distribution of the optical generation rate G_{opt} . Finally, drift-diffusion provides a solution of the electrical problem by using G_{opt} as a source term.

3 Results

Fig. 3 compares measurements and simulations of the electro-optic cutoff frequency at a reverse bias of 3 V and at different optical powers as measured at the laser output. (The optical power assigned in the simulations takes into account the losses between laser and detector due to fiber coupling and waveguide propagation, estimated to be 3 dB overall.)

In the figure, along with the simulation results (blue dots), are reported the mean values of the experimental electro-optic cutoff frequencies over five nominally identical devices (black dots), while the error bars represent the standard deviation of the measurements. An excellent match between measurements and simulations is observed for all the measured powers.

Increasing the optical power from -2 dBm to 3 dBm , the electro-optic cutoff frequency is reduced by more than 20%. This decrease can be explained in terms of a reduction of the carrier velocity due to a screening of the electric field in Ge by the photogenerated carriers. The magnitude of this effect is shown in Fig.

4, which reports the absolute value of the electric field evaluated along a 1D vertical cut, from metal to silicon substrate, near the beginning of the absorber. At low input optical power ($10\ \mu\text{W}$) the electric field is coincident with its profile in dark. On the contrary, at an optical power of $500\ \mu\text{W}$, the peak value of the electric field is reduced by a factor 3. This drop affects the device performance since the photogenerated carriers do not reach the saturation velocity, hence decreasing the electro-optic cutoff frequency.

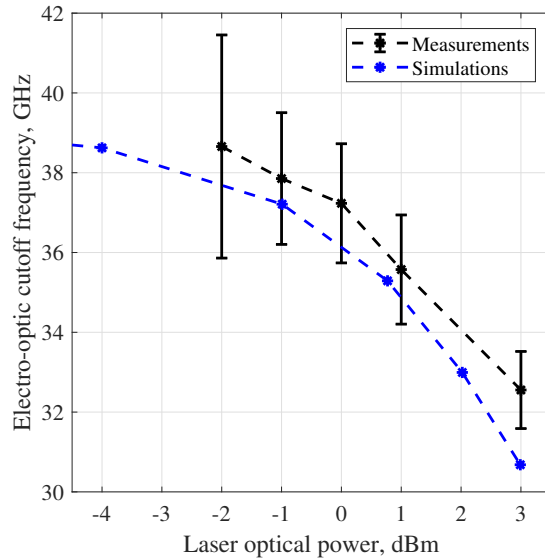


Fig. 3. Electro-optic cutoff frequency as a function of the optical power measured at the laser output.

4 Conclusions

The screening effect we have observed is a nonnegligible limitation to the performance of waveguide photodetectors in the O-band and should be taken into account in the device design. The excellent match demonstrated here between measurements and simulations suggest that the multiphysics 3D modeling approach provides a realistic description of this effect and can be used as an effective tool in the device optimization towards the new 200 Gbit/s applications [5,3].

5 Acknowledgments

This work was supported in part by Cisco Systems, Inc., under the Sponsored Research Agreement STACCATO.

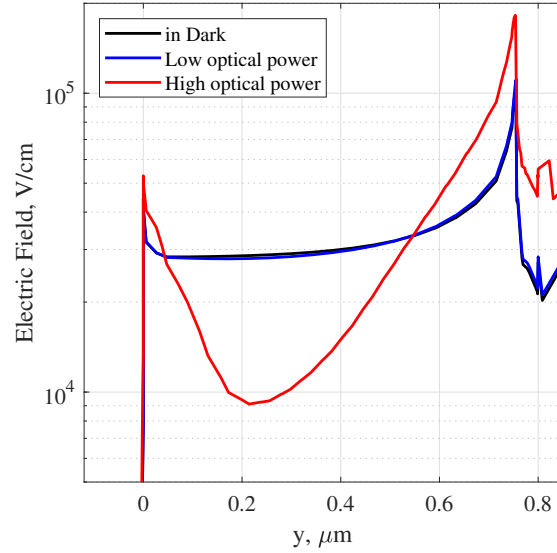


Fig. 4. Magnitude of the electric field in Ge along a 1D vertical cut between the center of the top metal contact and the silicon waveguide, at a distance of 1 μm from the front section of the absorber.

References

1. Alasio, M.G.C., Vallone, M., Tibaldi, A., Bertazzi, F., Namnabat, S., Adams, D., Gothoskar, P., Forghieri, F., Masini, G., Ghione, G., Goano, M.: Modeling the frequency response of vertical and lateral Ge-on-Si waveguide photodetectors: Is 3D simulation unavoidable? In: 2022 Conference on Lasers and Electro-Optics (CLEO). San Jose, CA (May 2022). https://doi.org/10.1364/CLEO_AT.2022.JW3A.28
2. Beling, A., Campbell, J.C.: High-speed photodiodes. *IEEE J. Select. Topics Quantum Electron.* **20**(6), 3804507 (Nov/Dec 2014). <https://doi.org/10.1109/JSTQE.2014.2341573>
3. Chen, D., Zhang, H., Liu, M., Hu, X., Zhang, Y., Wu, D., Zhou, P., Chang, S., Wang, L., Xiao, X.: 67 GHz light-trapping-structure germanium photodetector supporting 240 Gb/s PAM-4 transmission. *Photon. Res.* **10**(9), 2165–2171 (2022). <https://doi.org/10.1364/PRJ.455291>
4. Ghione, G.: *Semiconductor Devices for High-Speed Optoelectronics*. Cambridge University Press, Cambridge, U.K. (2009)
5. Hu, W., Xie, X., Xu, Q., Zhang, W., Song, H.: Research progress of SiGe hetero-junction photodetectors. In: Seventh Symposium on Novel Photoelectronic Detection Technology and Applications. vol. 11763, Proceedings of the SPIE, p. 11763A4. Kunming, China (Mar 2021). <https://doi.org/10.1117/12.2588373>
6. Keysight Technologies, Santa Rosa, CA: Lightwave Component Analyzer application notes (Dec 2017)

7. Palmieri, A., Vallone, M., Calciati, M., Tibaldi, A., Bertazzi, F., Ghione, G., Goano, M.: Heterostructure modeling considerations for Ge-on-Si waveguide photodetectors. *Opt. Quantum Electron.* **50**(2), 71 (Feb 2018). <https://doi.org/10.1007/s11082-018-1338-y>
8. Soref, R.: The past, present, and future of silicon photonics. *IEEE J. Select. Topics Quantum Electron.* **12**(6), 1678–1687 (Nov 2006). <https://doi.org/10.1109/JSTQE.2006.883151>
9. Soriano, V., Colace, L., Armani, N., Rossi, F., Ferrari, C., Lazzarini, L., Assanto, G.: Low-temperature germanium thin films on silicon. *Opt. Mater. Express* **1**(5), 856–865 (Sep 2011). <https://doi.org/10.1364/OME.1.000856>
10. Synopsys, Inc., Mountain View, CA: Sentaurus Device User Guide. Version N-2017.09 (Sep 2017)
11. Synopsys, Inc., Optical Solutions Group, Ossining, NY: RSoft FullWAVE User Guide, v2019.09 (2019)